# Morphology and Thermomechanical Properties of Epoxy Thermosets Modified with Polysulfone-*Block*-Polydimethylsiloxane Multiblock Copolymer

**Di Hu, Sixun Zheng**

*Department of Polymer Science and Engineering and State Key Laboratory of Metal Matrix Composites, Shanghai Jiao Tong University, Shanghai 200240, People's Republic of China*

Received 23 January 2010; accepted 19 June 2010
DOI 10.1002/app.32977
Published online 21 September 2010 in Wiley Online Library (wileyonlinelibrary.com).

**ABSTRACT:** Polysulfone-*block*-polydimethylsiloxane (PSF-*b*-PDMS) multiblock copolymer was synthesized via the Mannich polycondensation between phenolic hydroxyl-terminated polysulfone and aminopropyl-terminated polydimethylsiloxane in the presence of formaldehyde. The multiblock copolymer was characterized by means of nuclear magnetic resonance spectroscopy (NMR) and gel permeation chromatography (GPC) and used as a modifier to improve the thermomechanical properties of epoxy thermosets. Transmission electron microscopy (TEM) showed that the epoxy thermosets containing PSF-*b*-PDMS multiblock copolymer possesses the microphase-separated morphological structures. Depending on the content of the PSF-*b*-PDMS multiblock copolymer, the spherical particles with the size of 50–200 nm in diameter were dispersed into the continuous epoxy matrices. The measurement of static contact angles showed that with the inclusion of PSF-*b*-PDMS multiblock copolymer, the epoxy thermosets displayed the improved surface hydrophobicity. It is noted that the epoxy resin was significantly toughened in terms of the measurement of critical stress field intensity factor ($K_{1C}$).
 J Appl Polym Sci 119: 2933–2944, 2011

**Key words:** polysulfone-*block*-polydimethylsiloxane multiblock copolymer; epoxy resin; nanostructures; thermomechanical properties

## INTRODUCTION

Epoxy resins have widely been used as the high performance materials such as adhesives, matrices of composites, and electronic encapsulating materials. However, this class of thermosets is inherently of low impact resistance due to their high crosslinking density. During the past decades considerable efforts have been made to improve toughness of epoxy thermosets.[1–19] One of the successful routines to toughen epoxy thermosets is to incorporate polymeric modifiers into thermosetting matrix to form fine morphological structures. The effective polymer modifiers can be either elastomers[1–8] or thermoplastics.[9–19] Liquid rubbers such as carboxyl-terminated butadiene-acrylonitrile rubber (CTBN), amine-terminated butadiene-acrylonitrile rubber (ATBN) have been exploited to improve toughness of epoxy thermosets.[1–5] However, these liquid elastomers containing unsaturated bonds are prone to thermal instability and are of low oxidation resistance. Organosilicon elastomers (e.g., polydimethylsiloxane) possess the properties superior to the unsaturated elastomers, such as thermal stability, moisture resistance, and good electrical properties and thus are more advantageous modifiers. However, epoxies generally have poor compatibility with organosilicon elastomers due to their big difference in solubility parameter. As a consequence, the macroscopic phase separation often occurs in the blends of epoxies with polysiloxanes unless polysiloxanes were structurally modified to improve their affinity with epoxies. During the past decades, there has been ample literature to report the modification of epoxy thermosets by the use of organosilicon elastomers via a variety of approaches.[2,6–9] It has been demonstrated that the modification by the use of elastomers is mainly applied for the epoxy thermosets with lower crosslinking density.[1–8] Nonetheless, the toughness improvement of the epoxy thermosets with higher crosslinking density such as tetraglycidyldiaminodiphenylmethane (TGDDM) and novolac-type epoxy resin requires the incorporation of thermoplastics.[9–19] The formation of fine phase-separated morphology is

*Correspondence to:* S. Zheng (szheng@sjtu.edu.cn).
Contract grant sponsor: Natural Science Foundation of China; contract grant numbers: 20474038, 50873059.
Contract grant sponsor: National Basic Research Program of China; contract grant number: 2009CB930400.
Contract grant sponsor: Shanghai Synchrotron Radiation Facility; contract grant number: 08sro157.
Contract grant sponsor: Shanghai Leading Academic Discipline Project; contract grant number: B202.

crucial for the toughness improvement.[20] Some high performance polymers such as poly(ether imide) (PEI), poly(ether sulfone), and poly(ether ketone) have been employed to toughen epoxy thermosets.[9–19] Polysulfone (PSF) is a typical high performance polymer and it possesses the high glass transition temperature ($T_g$), good thermal stability and excellent mechanical strength. Owing to the excellent thermomechanical properties, PSF has been employed to modify epoxy thermosets.[13,14,21,22] It has been reported that no phase separation occurred when the thermosetting blends of epoxy resin with PSF were cured with 4,4-diaminodiphenylmethane.[23]

Recently, the modification of epoxy thermosets via the formation of nanostructures in the materials has increasingly attracted considerable interests.[24,25] Bates and coworkers[26–29] have investigated the effect of various nanostructures such as micelle, vesicles, or wormlike vesicles and found that the toughening of nanostructured thermosets are quite dependent on type and shape of dispersed nanophase and the interactions of the nanophases with thermosetting matrix, which could significantly affect either the debonding of the nanodomains (i.e., micelle or vesicles) from thermosetting matrix or crack deflection and frictional interlocking for the thermosets possessing the terraced morphology.[28] Pascault and coworkers[29] have reported maximum stress field intensity factors (i.e., $K_{1C}$) improvement of around two times by particles forming the "sphere-on-sphere" nanostructures in epoxy thermosets. Therefore, the control over the formation of nanostructures in thermosets using block copolymers has recently provoked considerable interests.[29–50] It has been identified that the formation of the nanostructures could follow either self-assembly[30,31] or reaction-induced microphase separation mechanism.[32,33] Bates and coworkers[30,31] have first reported the strategy of creating nanostructures via self-assembly approach. In the protocol, the precursors of thermosets act as the selective solvents of block copolymers and some self-assembly nanostructures such as lamellar, bicontinuous, cylindrical, and spherical structures are formed in the mixtures depending on the blend composition before curing reaction. These nanostructures can be further fixed via subsequent curing with introduction of hardeners. With an appropriate design of block copolymer architecture, the block copolymers self-organize to form ordered or disordered nanostructures. More recently, it was reported that ordered or disordered nanostructures in thermosets can be alternatively accessed via reaction-induced microphase separation (RIMS) mechanism.[32,33] In this mechanism, a part of subchains of block copolymers were demixed with the occurrence of polymerization whereas the other subchains still remain miscible with the matrix of the thermosets.

In this work, we explored to synthesize a novel multiblock copolymer consisting of PSF and PDMS blocks and then the multiblock copolymer was incorporated into epoxy to toughen the thermosets via the formation of nanostructures in the materials. The utilization of the multiblock copolymer and its modification of epoxy thermosets are based on the following considerations: (i) PSF was miscible with epoxy resin when the blends was cured with 4,4′-diaminodiphenylmethane (DDM)[23] and (ii) polydimethylsiloxane (PDMS) is immiscible with epoxy thermosets. It is expected that the microphase-separated morphology will be formed while the multiblock copolymer was incorporated into epoxy thermosets. Toward this end, we first report the synthesis and characterization of PSF-*b*-PDMS multiblock copolymer. Thereafter, the multiblock copolymer was incorporated into epoxy to obtain the modified thermosets. The morphology of the thermosets was investigated by means of transmission electron microscopy (TEM) and atomic force microscopy (AFM) and the fracture toughness of the materials is evaluated in terms of the measurement of critical stress intensity factors ($K_{1C}$).

## EXPERIMENTAL

### Materials

Diglycidyl ether of bisphenol A with the epoxide equivalent weight of 185–210 was obtained from Shanghai Resin, China. 4,4′-Dichlorodiphenylsulfone (DCDPS) was obtained from Yinsheng Chemical, Suzhou, China and it was recrystallized from toluene solution before use. 4,4′-Dihydroxylphenylisopropane is of analytically pure grade, purchased from Shanghai Reagent, Shanghai, China. Paraformaldehyde was purchased from Aldrich, USA. Aminopropyl-terminated polydimethylsiloxane was kindly supplied by Degussa, Germany and it has a quoted number-average molecular weight of $M_n = 2300$. Prior to use, it was dried via azeotropic distillation with anhydrous toluene. Unless specially indicated, all the chemicals such as 4,4′-diaminodiphenylmethane (DDM), potassium carbonate ($K_2CO_3$), and calcium hydride ($CaH_2$) were purchased from Shanghai Reagent, China. The solvents such as *N*-methyl-2-pyrrolidone (NMP) and toluene were obtained from commercial sources. Before use, NMP was dried over $CaH_2$ and then distilled under reduced pressure. Toluene was dried over sodium and then distilled; tetrahydrofuran, ethanol, and chloroform were used as received.

### Synthesis of phenolic hydroxyl-terminated polysulfone

Phenolic hydroxyl-terminated polysulfone [HO-PSF-OH] was prepared via the polycondensation

between excess 4,4′-dihydroxylphenylisopropane (BPA) and 4,4′-dichlorodiphenylsulfone (DCDPS) by following the literature method.[51,52] Typically, potassium carbonate ($K_2CO_3$) (15.73 g, 0.1138 mol) was added to a solution composed of BPA (22.24 g, 0.0976 mmol), DCDPS (25.05 g, 0.0871 mol), NMP (180 mL) and toluene (90 mL) and the solution was charged to a 500-mL flask equipped with $N_2$ inlet, condenser, and a magnetic stirrer. Under nitrogen atmosphere, the mixture was refluxed with vigorous stirring. With the polycondensation proceeding, the water produced was removed via azeotropic distillation using anhydrous toluene. To promote the dehydration of the system, the toluene was periodically distilled out using a Dean-Stark trap with an interval of 4 h. After five cycles, the reactive mixture was heated up to 175°C and the polymerization was carried out for additional 10 h. After cooling to room temperature, the inorganic salts were eliminated by filtration and the solution was dropped into a great amount of ethanol to obtain the precipitates. The precipitate (*viz*. the polymer) was dissolved with tetrahydrofuran and acidified with hydrochloric acid. The solution was concentrated using rotary evaporation and then was dropped into a great of ethanol to obtain the precipitates. The precipitates were dried at 50°C in a vacuum oven and 40.54 g polymer was obtained with the yield of 90.3%. $^1$H NMR ($CDCl_3$, ppm): 7.84 (4.9**H,** ortho protons of aromatic ring to sulfone group), 7.24 (4.9**H,** ortho protons of aromatic ring to isopropyl group), 7.09 (1**H,** meta protons of aromatic ring to isopropyl group at the end of chain), 7.00 (4.8**H**, ortho protons of aromatic ring to diphenylether linkage), 6.94 (4.9**H**, ortho protons of aromatic ring to the linkage of diphenylether), 6.75 (1**H,** ortho protons to aromatic to isopropyl group at the end of chain), 1.69 [7**H**, $C(CH_3)_2$ in chain], 1.65 [3**H**, $C(CH_3)_2$ at the end of chain]. The molecular weight of the polymer was estimated to be $M_n = 2448$ by means of $^1$H NMR spectroscopy.

### Synthesis of PSF-*b*-PDMS multiblock copolymer

Polysulfone-*block*-polydimethylsiloxane multiblock copolymer (PSF-*b*-PDMS) was synthesized through the polycondensation between phenolic hydroxyl-terminated polysulfone (HO-PSF-OH) and amino-terminated polydimethylsiloxane ($NH_2$-PDMS-$NH_2$), which was mediated with paraformaldehyde. Typically, to a three-necked flask equipped with a mechanical stirrer and a condenser, HO-PSF-OH (12.18 g, 5 mmol), $NH_2$-PDMS-$NH_2$ (11.47 g, 5 mmol) and a suspension of paraformaldehyde (0.78 g) in 15 mL toluene are charged and 100 mL anhydrous toluene was added. The reactive system was heated up to 100°C, at which the polymerization was carried out for 10 h. With the polymerization preceding, the viscosity of the system significantly increased. Cooled to room temperature, the reacted mixture was dropped into a great amount of ethyl ether to obtain the precipitates (i.e., the polymer). The polymer was resolved with tetrahydrofuran and the solution was redropped into ethyl ether to obtain the precipitates. The procedure was repeated for three times to purify the polymer. The resulting polymer was dried *in vacuo* at 30°C for 24 h before use. The $^1$H NMR ($CDCl_3$, ppm): 0.07 [4.50**H**, $CSi(CH_3)_2$], 1.7 [1.33**H**, $C(CH_3)_2$], 7.23 (1**H**, ortho protons of aromatic ring to isopropyl group), 6.97 (2.19**H**, *ortho* protons of aromatic ring to diphenylether linkage), 7.85 (1.04**H**, *ortho* protons of aromatic ring to sulfone group). GPC: $M_n = 24{,}700$ with the polydispersity of 2.24.

### Preparation of thermosets

The desired amount of PSF-*b*-PDMS multiblock copolymer was added to DGEBA with continuous stirring at 100°C until the mixtures became homogenous and transparent. Stoichiometric amount of 4,4′-diaminodiphenylmethane (DDM) with respect of DGEBA was added with continuous stirring until the full dissolution of the curing agent was attained. The mixtures were poured into Teflon molds and cured at 150°C for 2 h plus 180°C for 2 h.

### Measurements and characterization

#### Nuclear magnetic resonance spectroscopy (NMR)

The NMR measurements were carried out on a Varian Mercury Plus 400 MHz nuclear magnetic resonance spectrometer at 25°C. The polymer was dissolved with deuterated chloroform and the $^1$H NMR spectra were obtained with tetramethylsilane (TMS) as the internal reference.

#### Atomic force microscopy (AFM)

The samples were trimmed using a microtome machine, and the thickness of the specimens was about 70 nm. The morphological observation of the samples was conducted on a Nanoscope IIIa scanning probe microscope (Digital Instruments, Santa Barbara, CA) in tapping mode. A tip fabricated from silicon (125 μm in length with ca. 500-kHz resonant frequency) was used for scan, and the scan rate was 2.0 Hz.

#### Transmission electron microscopy (TEM)

Transmission electron microscopy analyses were performed on a JEOL JEM-2010 high resolution transmission electron microscopy at an acceleration

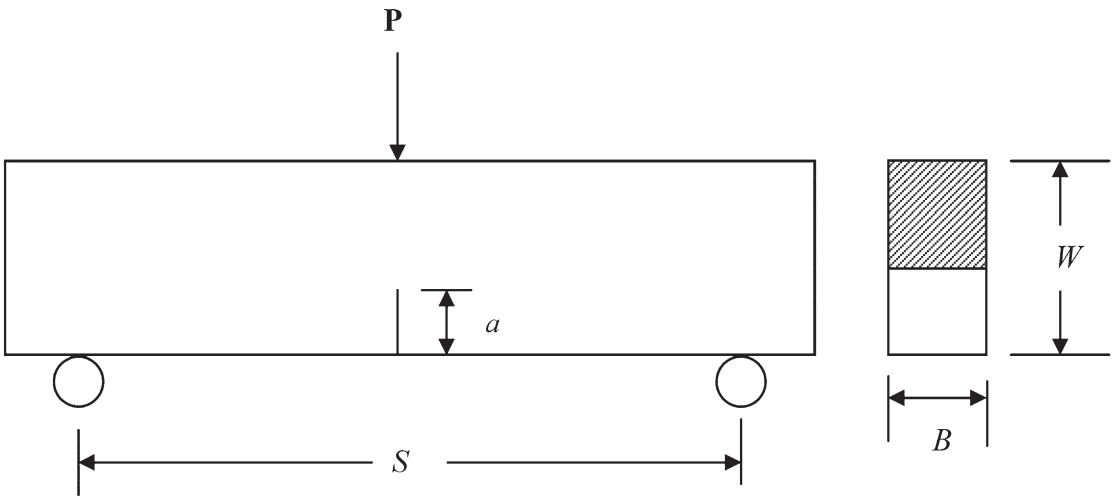


**Figure 1** Schematic diagram of three-point bending specimen for the measurement of critical stress intensity factor ($K_{IC}$).

voltage of 200 kV. The samples were trimmed using an ultramicrotome machine equipped with a diamond knife and then the ultrathin sections (ca. 70 nm) were placed on 200-mesh copper grids for observation.

### Differential scanning calorimetry (DSC)

Thermal analysis was performed on a Perkin–Elmer Pyris-1 differential scanning calorimeter in a dry nitrogen atmosphere. The instrument was calibrated with a standard Indium. The samples (about 10.0 mg in weight) were first heated up to 200°C and held at this temperature for 3 min to eliminate thermal history, followed by quenching to −70°C. To measure glass transition temperatures ($T_g$), a heating rate of 20°C $min^{-1}$ was used in all cases. Glass transition temperature ($T_g$) was taken as the midpoint of the heat capacity change.

### Gel permeation chromatography (GPC)

The molecular weights and molecular weight distribution of polymers were determined on a Waters 717 Plus autosampler gel permeation chromatography apparatus equipped with Waters RH columns and a Dawn Eos (Wyatt Technology) multiangle laser light scattering detector and the measurements were carried out at 25°C with *N,N*-dimethylformamide (DMF) as the eluent at the rate of 1.0 mL $min^{-1}$.

### Fracture toughness measurements

Fracture toughness was measured by the notched three-point bending test with a crosshead speed of 1.3 $mm^{-1}$ according to ASTM E399. The schematic diagram of the three-point bending specimens is shown in Figure 1. The critical stress intensity factors ($K_{1C}$) were calculated using the following equation:

$$K_{1C} = P_C S/BW^{3/2} f(a/W) \quad (1)$$

where $P_C$ is the load at crack initiation, $B$ is the thickness of the specimens, $S$ is the span width, $W$ is the width of the specimens and $a$ is the crack length. Central Vee-notches were machined. Before measurement, all the specimens were annealed at 80°C for 24 h and at least five successful measurements were used to obtain the average values of experiments.

## RESULTS AND DISCUSSION

### Synthesis of PSF-*b*-PDMS multiblock copolymer

The Mannich polycondensation among phenolic hydroxyl-terminated polysulfone, aminopropyl-terminated polydimethylsiloxane, and paraformaldehyde was employed to prepare polysulfone-*block*-polydimethylsiloxane multiblock copolymer (PSF-*b*-PDMS). The route of synthesis was shown in Schemes 1 and 2. In the first step, phenolic hydroxyl-terminated polysulfone (HO-PSF-OH) with the defined molecular weight was synthesized via the polycondensation between excess 4,4′-dihydroxylphenylisopropane (BPA) and 4,4′-dichlorodiphenylsulfone (DCDPS). The reaction was carried out in the presences of potassium carbonate ($K_2CO_3$) with methyl-2-pyrrolidone (NMP) as the solvent. By adjusting the molar ratio of BPA to DCDPS, the phenolic hydroxyl-terminated PSF with desired molecular weights can be prepared. With the $^1H$ NMR spectrum, the molecular weight of HO-PSF-OH can be estimated according to the ratio of proton integration intensity of the aromatic rings of BPA moieties at the ends of chain to that of BPA moiety in the chain (see Fig. 2). The molecular weight of HO-PSF-OH can be calculated in terms of the following equation:

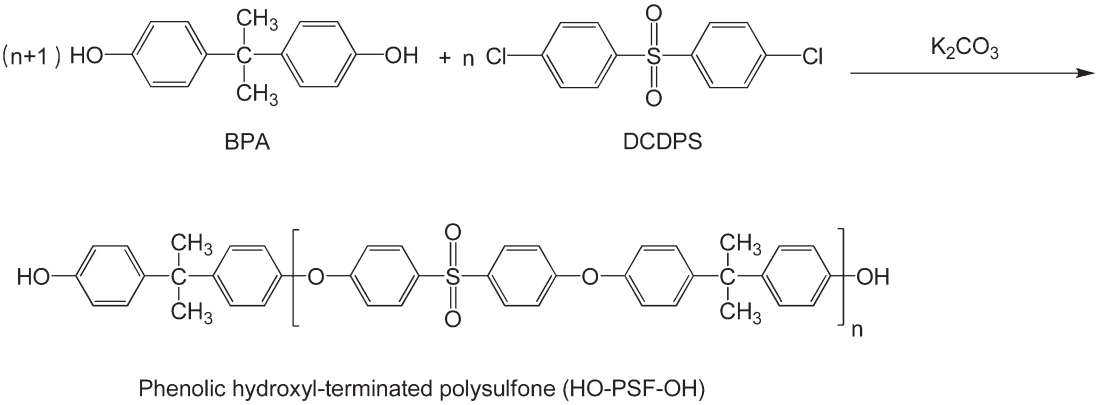


**Scheme 1** Synthesis of phenolic hydroxyl-terminated polysulfone.

$$M_n(\mathrm{PSF}) = M_n(\mathrm{BPA}) + A_c/A_a[M_n(\mathrm{BPA}) + M_n(\mathrm{DCDPS})] \quad (2)$$

where $A_c$ is the integration intensity of protons of aromatic rings to sulfone linkage in the chain (the resonance being denoted as "*c*") whereas $A_a$ the integration intensity of meta proton of aromatic ring to isopropyl group at the end of chain (the resonance being denoted as "*a*"); Both $M_n$(BPA) and $M_n$(DCDPS) are the molecular weights of 4,4′-dihydroxylphenylisopropane and 4,4′-dichlorodiphenyl sulfone, respectively. The molecular weight of HO-PSF-OH was calculated to be $M_n = 2448$, which is close to that of aminopropyl-terminated polydimethylsiloxane (*viz.* $M_n = 2300$). In the second step, the HO-PSF-OH was used to perform the Mannich polycondensation with the equimolar aminopropyl-terminated polydimethylsiloxane ($NH_2$-PDMS-$NH_2$) on the presence of formaldehyde to obtain the PSF-*b*-PDMS multiblock copolymer. It was observed that while the polycondensation proceeds the viscosity of the reactive system was significantly increased. The increased viscosity indicates that the Mannich polycondensation has been virtually carried out. Shown in Figure 3 is the $^1$H NMR spectrum of the resulting polymer. The signals of resonance at 0.1 and 0.4 ppm were assignable to the protons of methyl and methylene groups of PDMS block. The peaks in the ranges of 6.5–8.0 ppm was attributed to the resonance of the proton of the aromatic rings in PSF blocks. It is seen that the resonance assignable to the methylene protons of oxazine rings can be detected at 3.77 and 4.86 ppm. The $^1$H NMR spectroscopy indicates that the polymer combined the structural features from PSF and PDMS blocks. The molecular weight of the polymer was measured by means of gel permeation chromatography (GPC) and the GPC curve was shown in Figure 4. The GPC curve displayed a unimodal peak, suggesting that no detectible PSF and PDMS macromers in the resulting polymers, i.e., the Mannich polycondensation between the two macromers was performed to completion. The polymer possesses the high molecular weights of $M_n = 24{,}700$ with the polydispersity of $M_w/M_n = 2.24$. The results of $^1$H NMR spectroscopy and GPC indicate that the PSF-*b*-PDMS multiblock copolymer was successfully obtained. The PSF-*b*-PDMS multiblock copolymer was subjected to atomic force microscopy (AFM) to investigate the morphology of the copolymer and the AFM image was shown in Figure 5. The left hand side of the micrograph is topography image and the right the phase image. It is seen that the PSF-*b*-PDMS multiblock copolymer was microphase-separated. In terms of the difference in

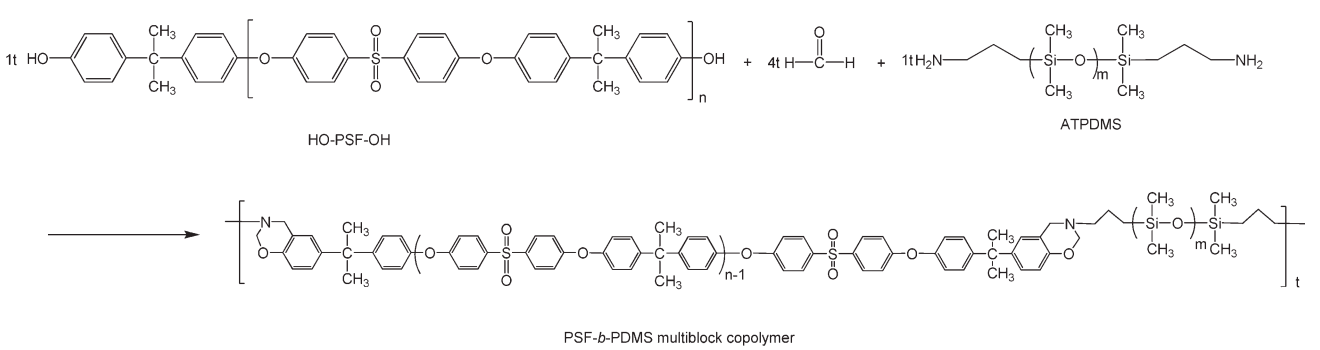


**Scheme 2** Polysulfone-*block*-polydimethylsiloxane multiblock copolymer (PSF-*b*-PDMS).

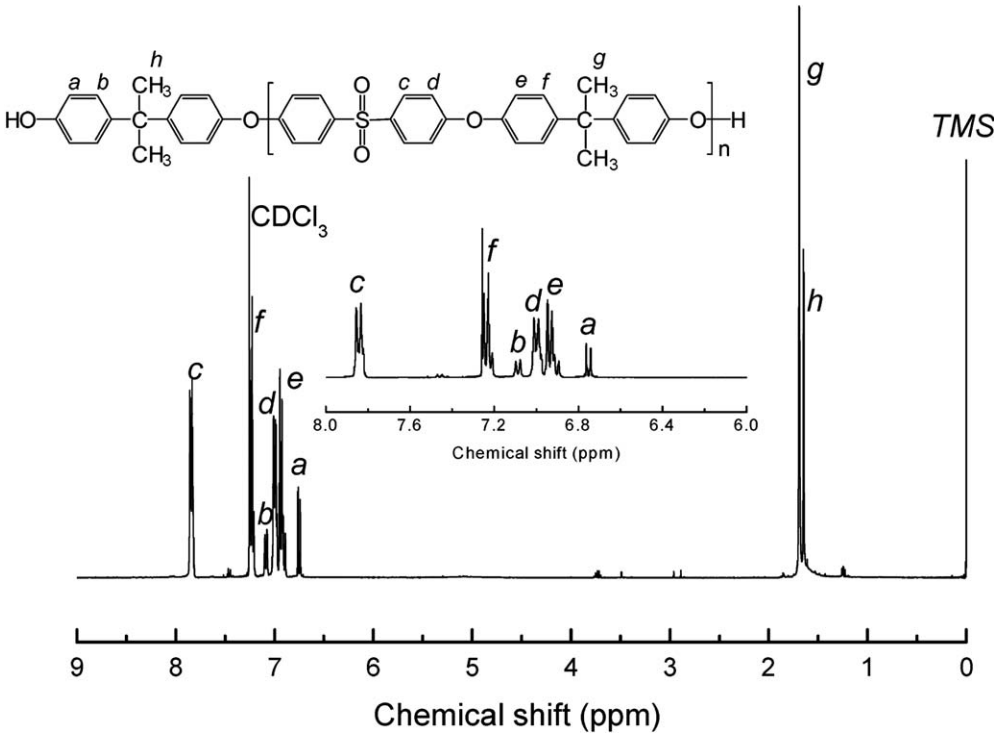


**Figure 2** [1]H NMR spectrum of phenolic hydroxyl-terminated polysulfone prepolymer (HO-PSF-OH).

viscoelastic properties of the blocks (*viz*. PSF and PDMS), the dark regions are attributed to the PDMS microdomains whereas the light regions to PSF microdoamons. The microphase-separated morphology of the multiblock copolymer is ascribed to the immiscibility of PSF block with PDMS blocks.

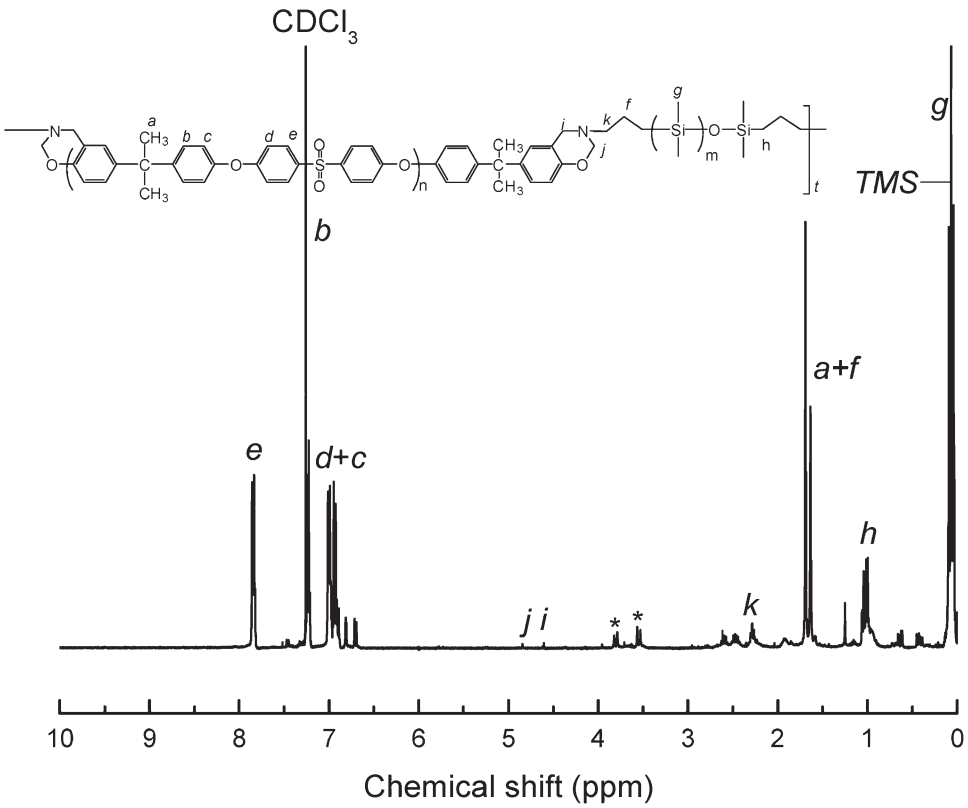


**Figure 3** [1]H NMR spectrum of polysulfone-*block*-polydimethylsiloxane multiblock copolymer (PSF-*b*-PDMS).

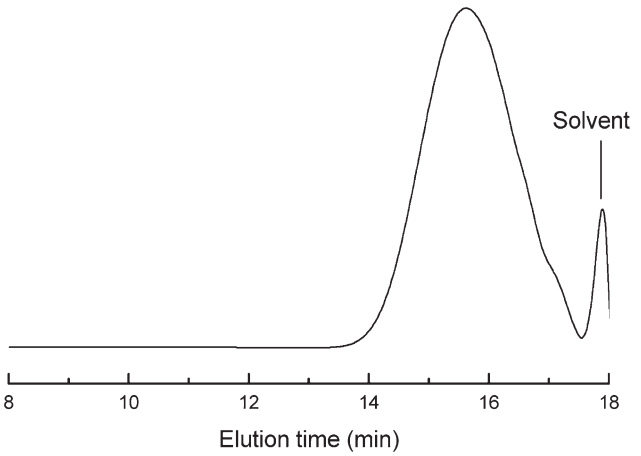


**Figure 4** GPC curve of PSF-*b*-PDMS multiblock copolymer.

### Epoxy thermosets containing PSF-*b*-PDMS

#### Morphology

The PSF-*b*-PDMS multiblock copolymer was incorporated into epoxy to prepare the nanostructured thermosets. Before curing, all the mixtures composed of diglycidyl ether of bisphenol A (DGEBA), 4,4′-diaminodiphenylmethane (DDM), and PSF-*b*-PDMS multiblock copolymer were homogenous and transparent, suggesting that no macroscopic phase separation occurred. After cured at elevated temperatures the epoxy thermosets containing PSF-*b*-PDMS multiblock copolymer were obtained with the content of PSF-*b*-PDMS up to 20 wt %. The morphology of the thermosets was examined by means of transmission electron microscopy (TEM). Shown in Figure 6 are the TEM micrographs of the thermosets containing various amount of PSF-*b*-PDMS multiblock copolymer. It is seen that in all the case, the thermosets containing PSF-*b*-PDMS multiblock copolymer were microphase-separated and the spherical particles with the size of 50–200 nm in diameter were dispersed into the continuous matrix. The quantity and size of these spherical microdomains increased with increasing the content of the multiblock copolymer [see Fig. 6(B) through 6(D)]. The enlarged micrograph of a spherical microdomain shows that the spherical particle turned out to be composed of some spherical nanoparticles with the size of 10–20 nm, which were dispersed into a continuous matrix (see Fig. 7). The nanoparticles in the big spherical particles are assignable to PDMS whereas the continuous matrix could be ascribed to the PSF blocks that were miscible with epoxy. This is the familiar salami morphology which has ever been found in high impact polystyrene containing polyisoprene (HIPS) via *in situ* polymerization.[53] It has been proposed that in HIPS the composite morphology resulted from several factors such as content of block copolymer, mechanical agitation rate and initiation rate of polymerization.[53] It is of interest to note that in the present case the similar morphology was formed in the thermosetting blends of epoxy with PSF-*b*-PDMS multiblock copolymer under the condition of quiescent curing.

It has been known that the formation of microstructures in thermosets containing amphiphilic block copolymers could follow either self-assembly[30,31] or reaction-induced microphase separation mechanisms.[32,33] For the mechanism of self-

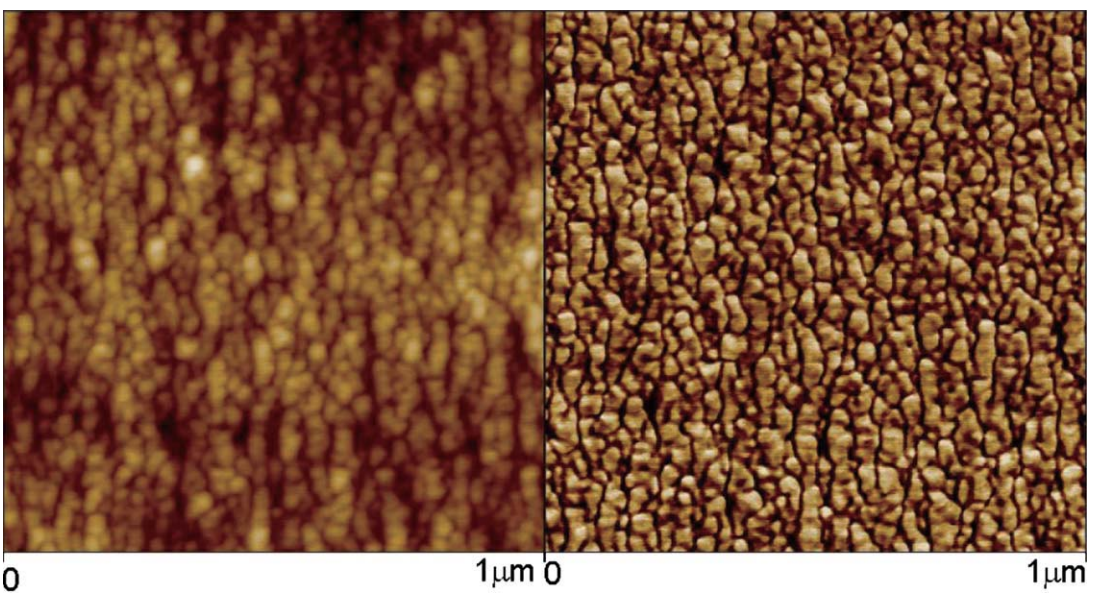


**Figure 5** AFM image of PSF-*b*-PDMS multiblock copolymer: Left: topography image; right: phase contrast image. [Color figure can be viewed in the online issue, which is available at wileyonlinelibrary.com.]

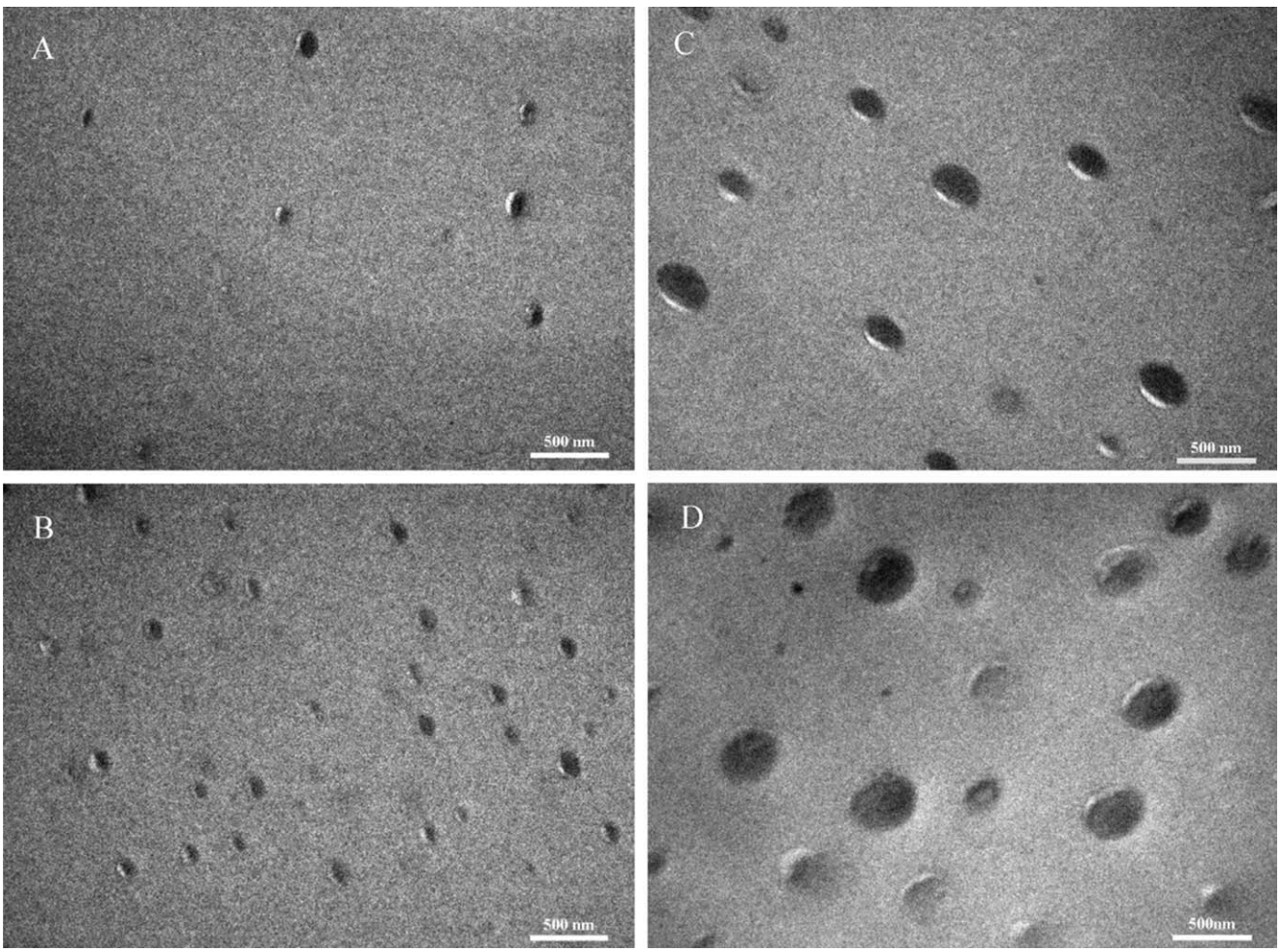


**Figure 6** TEM Micrographs of the epoxy thermosets containing (A) 5, (B) 10, (C) 15, and (D) 20 wt % PSF-*b*-PDMS multiblock copolymer.

assembly, the precursors of thermosets act as selective solvents of block copolymers and self-organized nanophases (i.e., micelle) are formed prior to curing. These disordered and/or ordered nanophases can further be fixed with the subsequent curing reaction.[30,31] For the formation of nanostructures via reaction-induced microphase separation mechanism, it is required that all the subchains of the block copolymer are miscible with precursors of thermosets before curing whereas only a part of subchains were separated out from the matrix of thermosets after curing. Therefore, it is crucial to know the miscibility of all the subchains with thermosets after and before curing reaction for the judgment of the formation mechanism of the nanostructures in thermosets containing amphiphilic block copolymers. In the present case, it has been known that the PSF block of the multiblock copolymer was miscible with the precursors of epoxy resin (*viz*. DGEBA and DDM) and also miscible with epoxy thermosets after curing.[23] As for the binary blends of epoxy resin and PDMS, it is recognized that the system are immiscible after and before curing reaction.[54] The immiscibility was responsible for the big difference in solubility parameters between epoxy and PDMS. The difference in miscibility between the two blocks (*viz*. PSF

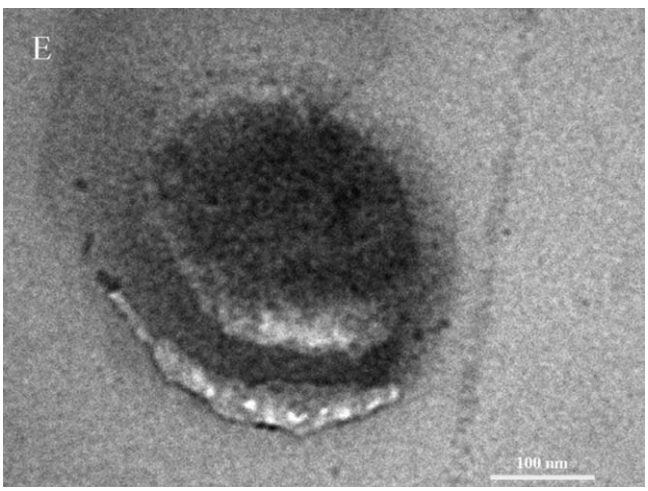


**Figure 7** Enlarged TEM micrograph of spherical microdomains in the epoxy thermosets containing 20 wt % PSF-*b*-PDMS multiblock copolymer.

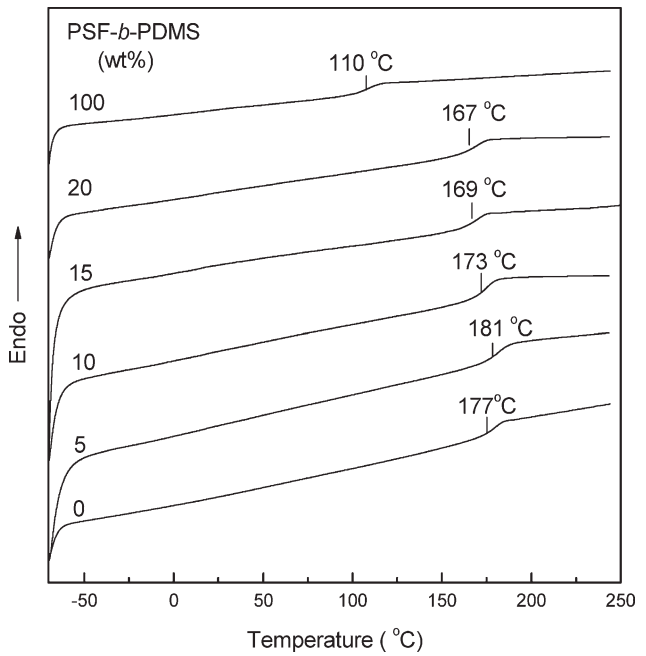


**Figure 8** DSC curves of control epoxy and the thermosets containing PSF-*b*-PDMS multiblock copolymer.

and PDMS) and epoxy precursors (*viz*. DGEBA and DDM) results in the formation of some self-organized microstructures in the mixtures of PSF-*b*-PDMS with epoxy before curing reaction. The self-organized nanophases would be fixed with the occurrences. However, it is noted that besides the thermosets containing 5 and 10 wt % PSF-*b*-PDMS multiblock copolymer in which the spherical particles were formed with the size of $\sim$ 50 nm [Fig. 6(A,B)], some spherical particles with the big size of 200 nm were detected [Fig. 6(C,D)]. This observation could be ascribed to the demixing of the miscible block (*viz*. PSF) induced by the reaction. It is proposed that with the occurrence of curing reaction, the PSF blocks that are initially miscible with epoxy could be expelled from the epoxy matrix resin. This expulsion leads to a "drying" or deswelling of the PSF block, leading to a subsequent reduction in interfacial curvature of PDMS nanodomains.[30,31] This phenomenon has been interpreted as a transition from equilibrium morphology to a chemically pinned metastable state as the crosslinking reaction progresses through the gel point.[30–31] It should be pointed out that this case is quite different from the occurrence of reaction-induced macroscopic phase separation since at the surface of the spherical particles the PSF subchains remained miscible with epoxy matrix, which was evidenced by the observation that the glass transition temperatures ($T_g$'s) of the epoxy matrices were decreased with increasing the content of the PSF-*b*-PDMS multiblock copolymer (see infra).

### Glass transition temperatures

The epoxy thermosets containing the PSF-*b*-PDMS multiblock copolymer were subjected to thermal analysis and the DSC curves of the thermosets were shown in Figure 8. The control epoxy thermoset displayed a single glass transition temperature ($T_g$) at about 177°C. For PSF-*b*-PDMS multiblock copolymer, the glass transition at about 110°C is assignable to PSF microdomains since the $T_g$ of PDMS was unable to detect in the temperature range of −70–250°C. It is noted that the $T_g$ value of the PSF microdomains is much lower than that of PSF with higher molecular weights (*viz*. 190°C) owing to the lower molecular weight (i.e., 2500). For the thermosets containing PSF-*b*-PDMS multiblock copolymer each DSC curve exhibited a single glass transition in the experimental range of temperature (−60–230°C). The glass transition is assignable to the matrix of the epoxy thermosets. While the content of PSF-*b*-PDMS multiblock copolymer is 5 wt % the $T_g$ of the thermoset is 181°C, which is slightly higher than that of the control epoxy. When the content of PSF-*b*-PDMS multiblock copolymer is more than 5 wt %, the $T_g$'s of the thermosets slightly decreased with increasing the content of PSF-*b*-PDMS multiblock copolymer. The decreased $T_g$'s are responsible for the miscibility of epoxy with PSF block. The plasticization of PSF block with the lower $T_g$ on the epoxy matrix resulted in the decreased $T_g$'s. In addition, it is possible that the benzoxazines linkage between PSF and PDMS

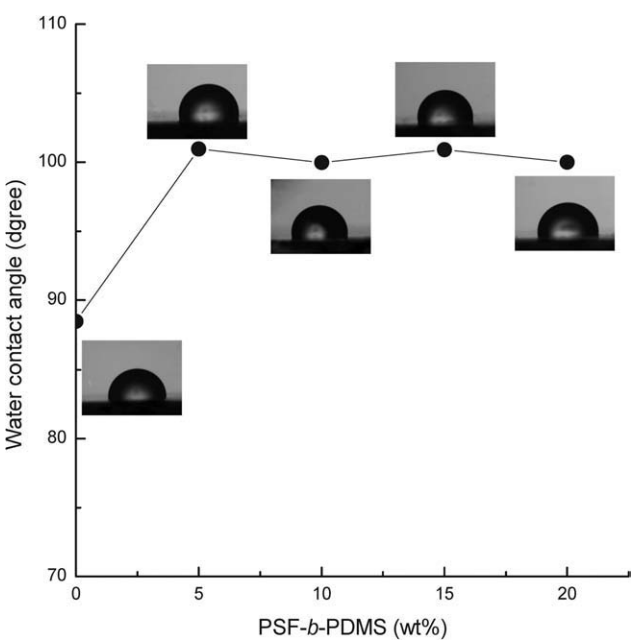


**Figure 9** Plot of surface water contact angle as a function of the content of PSF-*b*-PDMS multiblock copolymer for the thermosets. The images were taken from the measurement of surface contact angle with water as probe liquid.

**TABLE I**
**Static Contact Angles and Surface Free Energy of Epoxy Thermosets Containing PSF-*b*-PDMS Multiblock Copolymer**

| PSF-*b*-PDMS (wt %) | Static contact angle | | Surface free energy (mN × m$^{-1}$) | | |
|---|---|---|---|---|---|
| | $\theta_{H_2O}$ | $\theta_{\text{ethylene glycol}}$ | $\gamma_S^d$ | $\gamma_S^p$ | $\gamma_S$ |
| 0 | 88.5 ± 0.5 | 63.8 ± 0.7 | 21.9 | 4.72 | 26.7 |
| 5 | 100.9 ± 0.8 | 81.3 ± 0.4 | 2.64 | 14.6 | 17.3 |
| 10 | 100.0 ± 0.5 | 81.7 ± 0.3 | 3.44 | 13.0 | 16.5 |
| 15 | 100.9 ± 1.0 | 82.8 ± 1.0 | 3.21 | 12.8 | 16.0 |
| 20 | 100.1 ± 1.0 | 82.7 ± 0.5 | 3.83 | 11.9 | 15.7 |

blocks could participate in the crosslinking reaction of epoxy resin. This reaction could give rise to the decrease in crosslinking density of the thermosetting matrix and thus the $T_g$'s were decreased. It should be pointed out that the glass transitions observed in the present temperature range were only ascribed to the epoxy matrix which was miscible with the PSF subchains of the block copolymers and the $T_g$'s of PDMS microdomains ($\sim -123$°C) is beyond the temperature range of the DSC measurement. The present thermosetting system could follow the self-assembly mechanism.

## Surface properties

PDMS is an organosilicon polymer and possess low surface energy.[55] It is expected that the surface hydrophobilicity (or dewettability) of epoxy thermosets containing PSF-*b*-PDMS multiblock copolymer would be enhanced compared to the unmodified epoxy thermosets. The specimens of films for the samples were prepared via spin-coating technique. The free surfaces of the multiblock copolymer-containing thermosets were obtained and analyzed in terms of the measurement of static contact angle. Contact angles were measured with water and ethylene glycol as probe liquids and the plot of contact angles as a function of the content of PSF-*b*-PDMS multiblock copolymer was shown in Figure 9 and the results are summarized in Table I. The contact angle of pure epoxy thermoset was estimated with water to be about 88.5°. With the inclusion of 5 wt % PSF-*b*-PDMS multiblock copolymer the water contact angle of the thermoset was enhanced to about 100°. This increased contact angle indicates the hydrophobicity of materials was significantly increased; i.e., the surface energy of materials was reduced. It is noted that the contact angels of the thermosets remained at about 100°, i.e., the value of pure PDMS,[56,57] irrespective of the content of PSF-*b*-PDMS multiblock copolymer. This observation suggests that the surfaces of the thermosets could be enriched and saturated by PDMS chains. The surface free energies of the thermosets containing PSF-*b*-PDMS multiblock copolymers can be calculated according to the geometric mean model[58–60]:

$$\cos\theta = \frac{2}{\gamma_L}\left[\left(\gamma_L^d\gamma_S^d\right)^{\frac{1}{2}} + \left(\gamma_L^p\gamma_S^p\right)^{\frac{1}{2}}\right] - 1 \quad (3)$$

$$\gamma_S = \gamma_S^d + \gamma_S^p \quad (4)$$

where $\theta$ is contact angle and $\gamma_L$ is the liquid surface tension; $\gamma_L^p$ and $\gamma_L^d$ are the polar and dispersive components of $\gamma_L$, respectively. The calculated results of surface energy are also incorporated into Table I. The nonpolar component (i.e., $\gamma_S^d$) seems to be more sensitive than the polar component (i.e., $\gamma_S^p$) to the concentration of the PDMS, suggesting that the inclusion of PDMS significantly increased the distribution of the nonpolar groups on the surface energy of materials; i.e., the distribution of PDMS blocks on the surface was increased. The PDMS on the surface acted as a screening agent to reduce the surface energy of the multiblock copolymers. It is noticed that the values of the total surface free energy for the thermosets containing PSF-*b*-PDMS multiblock copolymers were significantly lower than that of the control epoxy thermoset. It should be pointed out that the surface hydrophobicity of the PDMS-containing PBa thermosets could be additionally changed in surface roughness (and/or surface topology) resulting from the formation of the microphase-separated structures.[55,61,62]

## Fracture toughness

The fracture toughness of the epoxy thermosets containing PSF-*b*-PDMS multiblock copolymer were evaluated in terms of three-point bending tests to measure the critical stress intensity factor ($K_{1C}$). The plots of $K_{1C}$ as a function of the content of the multiblock copolymer for the thermosets are presented in Figure 10. It is seen that the $K_{1C}$ values of all the thermosetting blends are significantly higher than that of the control epoxy, indicating that the epoxy thermoset was significantly toughened with the

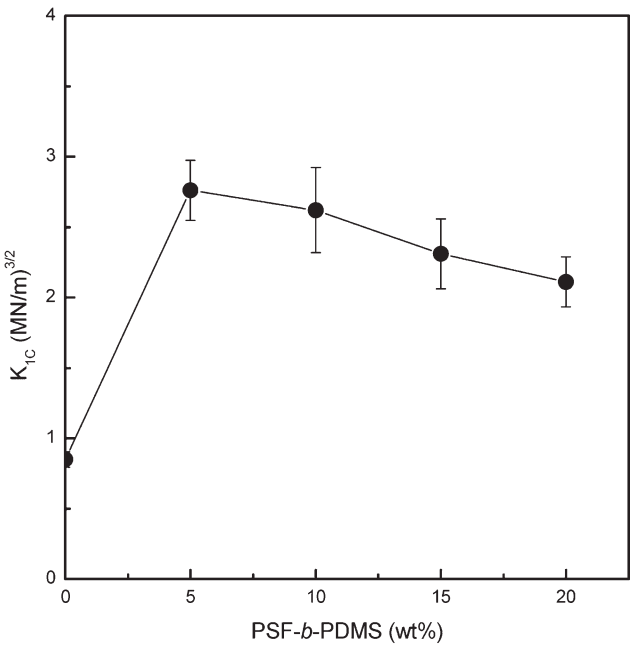


**Figure 10** Plots of $K_{1C}$ value as a function of the content of PSF-*b*-PDMS multiblock copolymers for the epoxy thermosets.

inclusions of the modifiers. The maximum $K_{1C}$ value is found about 2.8 MN/m$^{3/2}$ while the content of PSF-*b*-PDMS was 5 wt %, which is almost three times as that of the control epoxy. The values of $K_{1C}$ decreased with increasing the content of PSF-*b*-PDMS multiblock copolymer. Toughness improvement of epoxy thermosets with liquid rubbers has been extensively investigated during the past decades.[63,64] It is recognized that a combination of cavitation around the rubber particles with shear yielding in the matrix plays a major role in providing mechanism for energy dissipation.[27,28,42] In addition, microvoiding and tearing of the rubber particles may also occur. Compared to the thermosets modified with the liquid rubber, the toughness improvement of the thermosets containing block copolymers could display the following features: (i) the elastomeric component (*viz*. PDMS rubber) was homogenously dispersed in the thermosetting matrix at the nanometer scale, which will greatly optimize the interactions between the thermosetting matrix and the modifier; (ii) the interface interactions between thermosetting matrix and the PDMS nanodomains was significantly increased due to the miscibility of PSF blocks with the epoxy thermosets. It has been proposed that toughening of thermosets via the formation of nanostructures are quite dependent on type and shape of dispersed microdomains and the mechanisms could involving either the debonding of micelles (or vesicles) from epoxy matrix or crack deflection and frictional interlocking for the thermosets possessing the terraced morphology.[29] In the present case, the salami-like morphology were obtained when the concentration of PSF-*b*-PDMS is 10 wt % or higher and thus the energy-dissipation mechanisms could be related on the specific morphologies of epoxy thermosets modified with the triblock copolymer.

## CONCLUSIONS

Polysulfone-*block*-polydimethylsiloxane multiblock copolymer (PSF-*b*-PDMS) was synthesized via the Mannich polycondensation between hydroxyl-terminated polysulfone [HO-PSF-OH] and aminopropyl-terminated polydimethylsiloxane, which was mediated by paraformaldehyde. For the multiblock copolymer, the linkages of structures between PSF and PDMS blocks are benzoxazine rings. The multiblock copolymer was characterized by means of nuclear magnetic resonance spectroscopy (NMR) and gel permeation chromatography (GPC). The block copolymer was used as a modifier to improve the thermomechanical properties of epoxy thermosets. Transmission electron microscopy (TEM) showed that the epoxy thermosets containing PSF-*b*-PDMS multiblock copolymer possesses the microphase-separated morphological structures, in which the spherical particles with the size of 50–200 nm in diameter were dispersed into continuous epoxy matrices, depending on the content of PSF-*b*-PDMS multiblock copolymer. The spherical particles possessed microphase-separated microstructures. The measurement of static contact angles showed that with the inclusion of PSF-*b*-PDMS multiblock copolymer, the epoxy thermosets displayed the improved surface hydrophobicity. The fracture toughness of the nanostructured blends was evaluated in terms of the measurement of stress field intensity factor ($K_{1C}$) and it is noted that the epoxy resin was significantly toughened.

## References

1. Riew, C. K.; Rowe E. H.; Siebert A. R. Am Chem Soc Adv Chem Ser 1976, 154, 326.
2. Manson, J. A.; Hertzberg, R. W.; Connelly, G. M.; Hwang, J.; In Advances in Chemistry Series 211, Multicomponent Polymer Materials; Paul, D. R.; Sperling, L. M., Eds., Am. Chem. Soc., Washington D. C. 1986; p 300.
3. Yorkgitis, E. M.; Eiss, N. S.; Tran, C.; Wilkes, G. L.; McGrath, L. E. Am Chem Soc Adv Polym Sci 1985, 72, 70.
4. Yee, A. F.; Pearson, R. A. J Mater Sci 1986, 21, 2462.
5. Meijerink, J. I.; Eguchi, S.; Ogata, M.; Ishii, T.; Amagi, S.; Numata, S.; Sashima, H. Polymer 1994, 35, 179.
6. Zheng, S.; Wang, H.; Dai, Q.; Luo, X.; Ma, D. Macromol Chem Phys 1995, 196, 269.
7. Kemp, T. J.; Wilford, A.; Howarth, O. W.; Lee, T. C. P. Polymer 1992, 33, 1860.
8. Hisich, H. S.-Y. Polym Eng Sci 1990, 30, 493.
9. Bucknall, C. B.; Patridge, I. K. Polymer 1983, 24, 639.

10. Bucknall, C. B.; Gilbert, A. H. Polymer 1989, 30, 213.
11. Raghava, R. S. J Polym Sci B Polym Phys 1987, 25, 1017.
12. Hourston, D. J.; Lane, J. M. Polymer 1992, 33, 1397.
13. Hedrick, J. H.; Yilgor, I.; Wilkens, G. L.; McGrath, J. E. Polym Bull 1991, 13, 201.
14. Hedrick, J. H.; Yilgor, I.; Jurek, M.; Hedrick, J. C.; Wilkens, G. L.; McGrath, J. E. Polymer 1991, 13, 2020.
15. Raghava, R. S. J Polym Sci B Polym Phys 1988, 26, 65.
16. Gilbert, A. H.; Bucknall, C. B. Macromol Chem Phys Macromol Symp 1991, 45, 289.
17. Zheng, S.; Wang, J.; Guo, Q.; Wei, J.; Li, J. Polymer 1996, 37, 4667.
18. Song, X.; Zheng, S.; Huang, J.; Zhu, P.; Guo, Q. J Appl Polym Sci 2001, 79, 598.
19. Song, X.; Zheng, S.; Guo, Q. J Mater Sci 2000, 35, 5613.
20. Pascault, J. P.; Williams, R. J. J. In Polymer Blends; Paul, D. R.; Bucknall, C. B., Eds.; Wiley: New York, 2000; Vol. 1, p 379.
21. Cecere, J. A.; McGrath, J. E. Polym Prepr 1986, 27, 299.
22. Hedrick, J. L.; Jurek, M. J.; Yilgor, I.; McGrath, J. E. Polym Prepr 1985, 26, 293.
23. Huang, P.; Zheng, S.; Huang, J.; Guo, Q. Polymer 1997, 38, 5565.
24. Ruiz-Perez, L.; Royston, G. J.; Fairclough, J. P.; Pyan, A. J. Polymer 2008, 49, 4475.
25. Zheng, S. In Epoxy Polymers: New Materials and Innovations; Pascault, J. P.; Williams, R. J. J., Eds.; Wiley-VCH: Weinheim, 2010; p 79.
26. Dean, J. M.; Grubbs, R. B.; Saad, W.; Cook, R. F.; Bates, F. S. J Polym Sci B Polym Phys 2003, 41, 2444.
27. Wu, J.; Thio, Y. S.; Bates, F. S. J Polym Sci B Polym Phys 2005, 43, 1950.
28. Dean, J. M.; Lipic, P. M.; Grubbs, R. B.; Cook, R. F.; Bates, F. S. J Polym Sci B Polym Phys 2001, 39, 2996.
29. Rebizant, V.; Venet, A. S.; Tournillhac, F.; Girard-Reydet, E.; Navarro, C.; Pascault, J. P.; Leibler, L. Macromolecules 2004, 37, 8017.
30. Hillmyer, M. A.; Lipic, P. M.; Hajduk, D. A.; Almdal, K.; Bates, F. S. J Am Chem Soc 1997, 119, 2749.
31. Lipic, P. M.; Bates, F. S.; Hillmyer, M. A. J Am Chem Soc 1998, 120, 8963.
32. Meng, F.; Zheng, S.; Zhang, W.; Li, H.; Liang, Q. Macromolecules 2006, 39, 711.
33. Meng, F.; Zheng, S.; Li, H.; Liang, Q.; Liu, T. Macromolecules 2006, 39, 5072.
34. Mijovic, J.; Shen, M.; Sy, J. W. Mondragon, I. Macromolecules 2000, 33, 5235.
35. Grubbs, R. B.; Dean, J. M.; Broz, M. E.; Bates, F. S. Macromolecules 2000, 33, 9522.
36. Kosonen, H.; Ruokolainen, J.; Nyholm, P.; Ikkala, O. Macromolecules 2001, 34, 3046.
37. Guo, Q.; Thomann, R.; Gronski, W. Macromolecules 2002, 35, 3133.
38. Ritzenthaler, S.; Court, F.; Girard-Reydet, E.; Leibler, L.; Pascault, J. P. Macromolecules 2002, 35, 6245.
39. Ritzenthaler, S.; Court, F.; Girard-Reydet, E.; Leibler, L.; Pascault, J. P. Macromolecules 2003, 36, 118.
40. Rebizant, V.; Abetz, V.; Tournihac, T.; Court, F.; Leibler, L. Macromolecules 2003, 36, 9889.
41. Dean, J. M.; Verghese, N. E.; Pham, H. Q.; Bates, F. S. Macromolecules 2003, 36, 9267.
42. Zucchi, I. A.; Galante, M. J.; Williams, R. J. J. Polymer 2005, 46, 2603.
43. Thio, Y. S.; Wu, J.; Bates, F. S. Macromolecules 2006, 39, 7187.
44. Maiez-Tribut, S.; Pascault, J. P.; Soulé, E. R.; Borrajo, J.; Williams, R. J. J. Macromolecules 2007, 40, 1268.
45. Gong, W.; Zeng, K.; Wang, L.; Zheng, S. Polymer 2008, 49, 3318.
46. Serrano, E.; Tercjak, A.; Kortaberria, G.; Pomposo, J. A.; Mecerreyes, D.; Zafeiropoulos, N. E.; Stamm, M.; Mondragon, I. Macromolecules 2006, 39, 2254.
47. Sinturel, C.; Vayer, M.; Erre, R.; Amenitsch, H. Macromolecules 2007, 40, 2532.
48. Ocando, C.; Serrano, E.; Tercjak, A.; Pena, C.; Kortaberria, G.; Calberg, C.; Grignard, B.; Jerome, R.; Carrasco, P. M.; Mecerreyes, D.; Mondragon, I. Macromolecules 2007, 40, 4068.
49. Xu, Z.; Zheng, S. Macromolecules 2007, 40, 2548.
50. Meng, F.; Xu, Z.; Zheng, S. Macromolecules 2008, 41, 1411.
51. Pospiech, D.; Haudler, L.; Komber, H.; Voict, D.; Jehnichen, D.; Janke, A.; Baier, A.; Eckstein, K.; Bohme, F. J Appl Polym Sci 1996, 62, 1819.
52. Zhang, Y.; Chung, I. S.; Huang, J.; Matyjaszewski, K.; Pakula, T. Macromol Chem Phys 2005, 206, 33.
53. Patricia Leal G.; Asua, J. M. Polymer 2009, 50, 68.
54. Xu, Z.; Zheng, S. Polymer 2007, 48, 6134.
55. Zhang, X.; Shi, F.; Yu, X.; Liu, H.; Fu, Y.; Wang, Z. Q.; Jiang, L.; Li, X. Y. J Am Chem Soc 2004, 126, 3064.
56. Seo, J.-H.; Matsuno, R.; Konno, T.; Takai, M.; Ishihara, K. Biomaterials 2008, 29, 1367.
57. Zhang, X.; Lin, G.; Kumar, S. R.; Mark, J. E. Polymer 2009, 5, 5414.
58. Kaelble, D. H.; Uy, K. C. J Adhes 1970, 2, 50.
59. Kaelble, D. H. Physical Chemistry of Adhesion; Wiley-Interscience: New York, 1971.
60. Adamson, A. W. Physical Chemistry of Surfaces, 5th ed.; Wiley-Interscience: New York, 1990.
61. Feng, L.; Li, S.; Li, Y.; Li, H.; Zhang, L.; Zhai, J.; Song, Y.; Liu, B.; Jiang, L.; Zhu, D. Adv Mater 2002, 14, 1857.
62. Han, J. T.; Xu, X. R.; Cho, K. W. Langmuir 2005, 21, 6662.
63. Pearson, R. A.; Yee, A. F. J Mater Sci 1986, 21, 2475.
64. Thomas, R.; Abraham, J.; Thomas, P. S.; Thomas, S. J Polym Sci B Polym Phys 2004, 42, 2531.